European Journal of Radiology 116 (2019) 106–115

Contents lists available at ScienceDirect

European Journal of Radiology

journal homepage: www.elsevier.com/locate/ejrad

Systematic review and meta-analysis of MRI signs for diagnosis of idiopathic intracranial hypertension

Robert M. Kwee[a,*], Thomas C. Kwee[b]

[a] Department of Radiology, Zuyderland Medical Center, Henri Dunantstraat 5, 6419 PC, Heerlen/Sittard/Geleen, the Netherlands
[b] Department of Radiology, Nuclear Medicine and Molecular Imaging, University Medical Center Groningen, University of Groningen, the Netherlands

ARTICLE INFO

Keywords:
Idiopathic intracranial hypertension
Pseudotumor cerebri
Magnetic resonance imaging
Diagnostic accuracy
Systematic review
Meta-analysis

ABSTRACT

Objective: To systematically review the potential value of MRI signs in the assessment of intracranial hypertension (IIH).
Methods: MEDLINE and Embase were systematically searched for original studies investigating the accuracy of MRI signs in diagnosing IIH. Methodologic quality of included studies was assessed. Sensitivity and specificity were pooled with a bivariate random-effects model.
Results: Twenty-one studies, comprising a total of 724 patients with IIH, were included. All studies had a case-control design. "Empty" sella (11 studies), posterior displacement of pituitary stalk (2 studies), meningoceles (2 studies), posterior globe flattening (8 studies), optic nerve head protrusion (6 studies), optic nerve enhancement (3 studies), optic nerve sheath distension (12 studies), optic nerve tortuosity (7 studies), slit-like ventricles (4 studies), tight subarachnoid spaces (3 studies), and inferior position of cerebellar tonsils (4 studies) had pooled sensitivity ranging between 6.1% and 68.6%, and pooled specificity ranging between 84.0% and 99.2%. Transverse sinus stenosis (8 studies) had pooled sensitivity of 84.4%; (95% CI: 65.9–93.9%) and pooled specificity of 94.9% (95% CI: 91.7–96.9%).
Conclusion: "Empty" sella, posterior pituitary stalk displacement, meningoceles, posterior globe flattening, optic nerve head protrusion, optic nerve enhancement, optic nerve sheath distension, optic nerve tortuosity, slit-like ventricles, tight subarachnoid spaces, and inferior position of cerebellar tonsils have overall high specificity but low sensitivity. Transverse sinus stenosis appears to be the most useful sign, because it has high specificity and fairly high sensitivity.

1. Introduction

Idiopathic intracranial hypertension (IIH) is a clinical syndrome characterized by raised intracranial pressure (ICP), without a detectable cause and absence of hydrocephalus [1]. The exact cause is still unclear [2]. Headache and visual impairment are the most common symptoms and blindness occurs in 10% of cases [1]. In young adult women with overweight, incidence is 15–19 cases per 100,000 persons in the USA [3]. Because IIH is associated with obesity [4], its incidence is likely to increase with increasing global obesity [5]. Diagnosis relies on clinical symptoms, absence of hydrocephalus, intracranial mass, structural, or vascular lesion on imaging, raised cerebrospinal fluid (CSF) pressure measured by lumbar puncture, and normal CSF composition.[1] However, IIH is frequently overdiagnosed, in as much as 39.5% of patients referred for presumed IIH [6]. The most common diagnostic error is inaccurate funduscopic examination [6], which can be challenging [7]. Moreover, IIH can also occur without papilledema [8]. In these cases, diagnosis may strongly depend on MRI. Reported MRI signs that may be helpful for the diagnosis of IIH include "empty" sella, posterior globe flattening, optic nerve sheath distension with or without optic nerve tortuosity, and transverse sinus stenosis [8]. However, incidental finding of potential nonspecific MRI signs may lead to overdiagnosis of IIH and resultant excessive additional tests, including lumbar punctures [7], and unnecessary treatment. To our knowledge, the potential value

* Corresponding author.
E-mail address: rmkwee@gmail.com (R.M. Kwee).

https://doi.org/10.1016/j.ejrad.2019.04.023
Received 31 January 2019; Received in revised form 6 April 2019; Accepted 29 April 2019

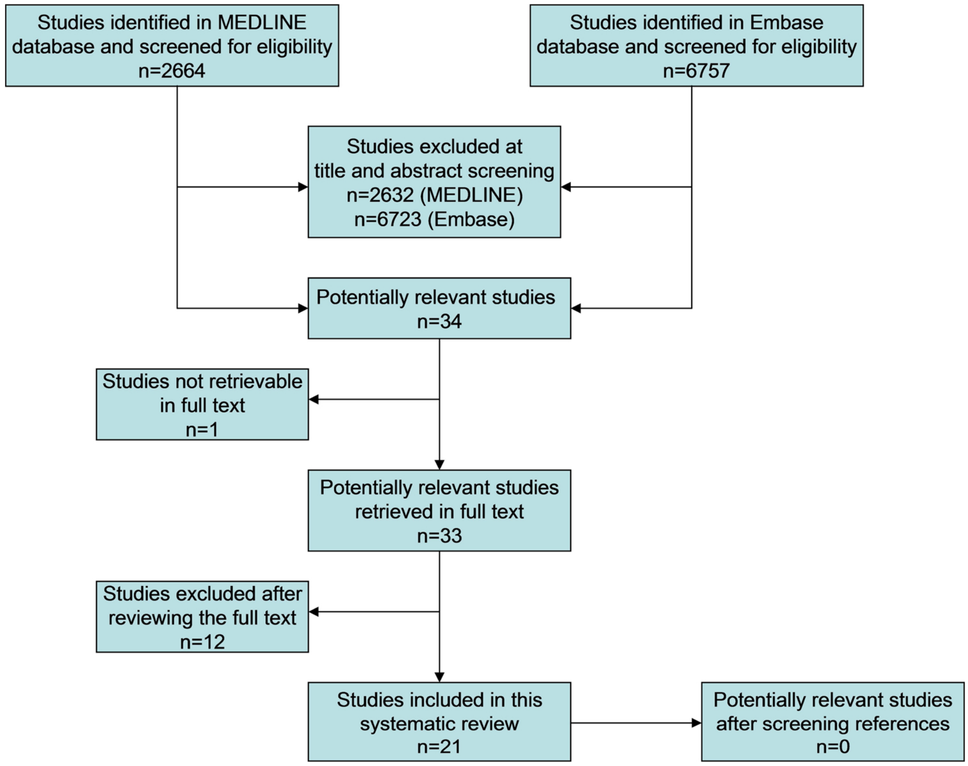

Fig. 1. Flowchart of the study selection process.

of MRI has not been systematically investigated yet. Therefore, the purpose of this study was to systematically review and meta-analyze the potential value of MRI signs in the assessment of IIH.

2. Materials and methods

2.1. Data sources

MEDLINE and Embase was searched for publications on the accuracy of MRI in diagnosing IIH. The search terms ((intracranial AND hypertension) OR (pseudotumor AND cerebri)) AND (magnetic resonance OR MR imaging OR MRI OR magnetic resonance tomography OR nuclear magnetic resonance OR NMR) were used. The search was updated until November 24, 2018. Bibliographies of studies which remained after the selection process were screened for potentially suitable references.

2.2. Study selection

Original studies investigating the accuracy of MRI signs in diagnosing IIH were eligible for inclusion. Studies involving < 10 IIH patients were excluded. Studies only investigating patients with secondary intracranial hypertension (i.e. intracranial hypertension with an identifiable cause) were excluded. Studies which provided insufficient data to construct a 2×2 contingency table to calculate sensitivity and specificity were also excluded. When data were presented in more than one article, the article with the largest number of patients was chosen. With use of aforementioned selection criteria, titles and abstracts of retrieved studies were reviewed. Full-text versions of potentially eligible articles were retrieved. Full-text articles were then reviewed to definitively determine if the study was eligible for inclusion.

2.3. Study data extraction

For each included study, principle characteristics, and true positive, false positive, false negative, and true negative values of MRI signs in diagnosing IIH were extracted.

2.4. Study quality assessment

Study quality was assessed by using the Quality Assessment of Diagnostic Accuracy Studies 2 (QUADAS-2) tool, which comprises 4 key domains: "patient selection", "index test", "reference standard", and "flow and timing" [9].

2.5. Statistical analyses

Sensitivity and specificity of individual MRI signs were calculated and pooled using a bivariate random-effects model [10], if supported by abstracted data from at least two studies. A Chi-squared test was performed to test for heterogeneity. Potential sources for heterogeneity were explored by assessing whether certain covariates significantly influenced the relative diagnostic odds ratio (RDOR) [11]. Pre-specified covariates were study size (< 30 vs. ≥ 30 patients with IIH [30 was the median]), type of control subjects ("normal" volunteers vs. patients with normal brain MRI findings), and pediatric (< 18 years) vs. adult (≥18 years) patients. Subgroup analyses were only performed when there were at least 4 studies per subgroup [12]. Statistical analyses were performed using Meta-analysis of Diagnostic Accuracy Studies package in R software [13,14].

Table 1
Principal study characteristics.

Study	Publication year, country of origin	Number of patients with IIH, age and sex	Definition of IIH	Number of control subjects, age and sex	Description of control subjects
Pellerin et al. [15]	2018, France	24, mean age 28.5 years (± 8.4), 21 females	Revised modified Dandy criteria [8]	24, mean age 31.6 years (± 7.4), 21 females	NS
Delen et al. [18]	2018, Turkey	28, mean age 28.5 years (range 18-60), 24 females	Modified Dandy criteria [61]	20, mean age 33 years (range 24-49), 18 females	Subjects with symptoms other than those of increased ICP and normal neurological examination.
Morris et al. [20]	2017, USA	63, mean age 31.6 years (± 10.6), 58 females	Revised modified Dandy criteria [8]	96, mean age 35.5 years (± 9.8), 72 females	Patients with migraine or headache not otherwise specified, and no obvious intracranial pathology.
Carvalho et al. [21]	2017, Brazil	32, mean age 34.4 years (range 19-58), 31 females	Modified Dandy criteria [61]	31, 32.4 years (range 20-52), 29 females	Patients with no diseases that could increase ICP, no IIH symptoms, no suspicion of venous abnormality, and normal brain MRI findings.
Zur et al. [24]	2017, Israel	38, mean age 33 years (± 10), 34 females	Modified Dandy criteria [61]	30, mean age 33 years (± 11), 27 females	Patents with normal brain MRI (indications: suspicion of vasculitis, headaches, vessel irregularity on CTA, trigeminal neuralgia, paresthesia, blurred vision, suspicion of vascular malformation, eclampsia, suspicion of intracranial hypotension)
Görkem et al. [26]	2015, Turkey	25, median age 12 years (range 1-17), 9 women	NS	30, median age 11 years (range 4-17), 16 women	Patients with normal brain MRI (indications: various reasons such as headache or instability) and no symptoms of increased ICP or secondary intracranial hypertension.
Bialer et al. [30]	2014, USA	79, median age 28 years (range 34-36), 77 females	Modified Dandy criteria [61]	76, median age 33.4 years (range 30-40), 62 females	Patients without headache or visual complaints and normal brain MRI (indications: sensory disturbances, peripheral neuropathies, seizures, metastatic screening)
Ranganathan et al. [31]	2013, USA	10, mean age 28.4 years (± 9.8), 10 females	Modified Dandy criteria [61]	11, mean age 30.8 years (+/-8.5), 11 females	Healthy young women
Hoffmann et al. [32]	2013, Germany	25, mean age 37.0 years (± 13.7), 22 females	International Headache Society criteria [62]	25, mean age 37.9 years (+/-11.8), 22 females	Healthy volunteers
Aiken et al. [33]	2012, USA	43, NS, 42 females	Clinical diagnosis of IIH with CSF opening pressure > 20 cm H2O in nonobese and > 25 cm H2O in obese patients.	44, mean age 40 years (range 18-61), 27 females	Patients with normal brain MRI scanned for other reasons.
Butros et al. [34]	2012, USA	44, NR, 43 females	Modified Dandy criteria [61]	44, NR, 43 females	Patients with normal brain MRI (indications: headaches, dizziness, weakness) and no clinical findings of IIH.
Maralani et al. [35]	2012, Canada	43, mean age 34.3 years (range 17-63), 39 females	Modified Dandy criteria [61]	43, mean age 37.2 years (range 18-65), 28 females	Patients with normal brain MRI (indications: headaches, possible optic disc swelling, eclampsia, suspected intracranial hypotension, hyperdense venous sinuses on brain CT, tinnitus)
Degnan et al. [37]	2011, USA	46, mean age 37.9 years (range 21-66), 45 females	Based on clinical syndrome, papilledema at funduscopic examination, and elevated CSF opening pressure.	46, NR, 45 females	Patients with normal brain MRI (indications: evaluation after trauma or to rule out cerebrovascular accident)
Lim et al. [38]	2010, UK	23, mean age 8 years (± 3.45), 10 females	Modified Dandy criteria [61]	20, mean age 8 years (± 4.7), 10 females	Children with normal brain MRI (indications: variety of other reasons)
Lingawi et al. [39]	2009, Saudi Arabia	45, mean age 32 years, 29 females	Modified Dandy criteria [61]	19, mean age 29.5 years, 10 females	Healthy volunteers
Agid et al. [41]	2006, Canada	30, mean age 37.2 years (range 18-66), 22 females	Headache, papilledema, CSF opening pressure > 20 cm H2O, normal CSF constituents, no condition or medication associated with intracranial hypertension, normal brain MRI, and no evidence of sinovenous thrombosis.	56, mean age 59.6 years (range 23-81), 28 females	Patients screened for intracranial metastatic disease with no overt signs or symptoms of neurological disease and normal brain MRI.
Higgins et al. [43]	2004, UK	20, mean age 30 years (range 16-69), 17 females	Syndrome of raised ICP, no hydrocephalus or mass on imaging, no evidence of sinovenous thrombosis, and normal CSF constituents.	40, mean age 30 years (range 14-71), 34 females	Normal volunteers
Yuh et al. [45]	2000, USA	40, mean age 25.8 years (range 9-49), 32 females	NS	23, mean age 32 years (range 22-50), 9 females	Normal subjects. Pregnant and postpartum women were excluded.
Farb et al. [46]	2003, Canada	29, 37.2 years (range 18-66), 21 females	Headache, papilledema, CSF opening pressure > 20 cm H2O, normal CSF constituents, no condition or medication associated with intracranial hypertension, normal brain MRI, and no evidence of sinovenous thrombosis.	59, 60.3 years (range NR), 28 females	Patients screened for intracranial metastatic disease with no overt signs or symptoms of neurological disease and normal brain MRI.

(*continued on next page*)

Table 1 (*continued*)

Study	Publication year, country of origin	Number of patients with IIH, age and sex	Definition of IIH	Number of control subjects, age and sex	Description of control subjects
Brodsky et al. [47]	1998, USA	20, age range 3-66 years, 18 females	Elevated ICP signs and symptoms, elevated CSF opening pressure, normal CSF, normal neurologic examination (except 6th nerve palsy), and no hydrocephalus or mass on imaging.	20, NR, NR	Subjects with no clinical evidence of elevated ICP, visual dysfunction, or disc elevation.
Gass et al. [48]	1996, UK	17, mean age 32 years (range 18-50), 15 females	IIH symptoms. Confirmation of IIH by elevated CSF opening pressure, imaging and additional diagnostic tests when appropriate.	15, range 20-41 years, 9 females	Healthy individuals without more than one headache per month.

CT: computed tomography.
CTA: computed tomography angiography.
IIH: idiopathic intracranial hypertension.
ICP: intracranial pressure.
MRI: magnetic resonance imaging.
NR: not reported.
NS: not specified.

3. Results

3.1. Literature search

The study selection process is displayed in Fig. 1. Thirty-four studies were potentially eligible for inclusion [15–48]. One study was excluded because the full-text version could not be retrieved [42]. After reviewing the full text of the remaining 33 studies, 11 studies were excluded because accuracy of MRI in diagnosing IIH was not investigated or reported [16,17,19,22,23,25,28,29,36,40,44], and one study [27] was excluded because data were also used in another article from the same group, comprising a larger number of patients [32]. Eventually, 21 studies were included, published between 1989 and 2018 [15,18,20,21,24,26,30–35,37,38,41–43,45,16–48].

Median number of patients with IIH per included study was 30 (range 10–79), with a total of 724 patients with IIH included in this systematic review. Median percentage of female patients with IIH per included study was 88.2 (range 36–100). Principal characteristics of the included studies are displayed in Table 1. The interpreter(s) of MRI are displayed in Table 2.

3.2. Methodologic quality assessment

QUADAS-2 assessments are displayed in Table 3 and summarized in Fig. 2. Risk of bias with respect to patient selection was rated "high" in all 21 studies [15,18,20,21,24,26,30–35,37,38,41–43,45–48], because a case-control design was used. Risk of bias with respect to index test was rated “high” in 14 studies [15,21,24,26,31–33,35,37,39,43,45,46,48], because diagnostic criterion of one or more of the MRI signs was not prespecified. Risk of bias with respect to reference standard was rated “unclear” in all 21 studies [15,18,20,21,24,26,30–35,37,38,41–43,45–48], because it was unclear whether the reference standard was interpreted without knowledge of the results of the index test. Furthermore, in two studies the definition of IIH was not specified [26,45]. There were no applicability concerns.

3.3. Diagnostic performance

Various MRI signs were investigated by the included studies (Table 4). "Empty" sella (11 studies), posterior displacement of pituitary stalk (2 studies), meningoceles (2 studies), posterior globe flattening (8 studies), optic nerve head protrusion (6 studies), optic nerve enhancement (3 studies), optic nerve sheath distension (12 studies), optic nerve tortuosity (7 studies), slit-like ventricles (4 studies), tight subarachnoid spaces (3 studies), and inferior position of cerebellar tonsils (4 studies) had pooled sensitivity ranging between 6.1% and 68.6%, and pooled specificity ranging between 84.0% and 99.2%. Transverse sinus stenosis (8 studies) had pooled sensitivity of 84.4%; (95% confidence interval [CI]: 65.9–93.9%) and pooled specificity of 94.9% (95% CI: 91.7–96.9%). Accuracy of other MRI signs (Meckel's cave enlargement, Meckel’s cave narrowing, cavernous sinus diameter, DWI bright spot at optic fundus, and papilledema) were only reported by single studies (see Table 4).

Only specificities of optic nerve head protrusion ($P = 0.745$), optic nerve tortuosity ($P = 0.560$), transverse sinus stenosis ($P = 0.561$), and specificity ($P = 0.498$) and sensitivity ($P = 0.493$) of slit-like ventricles were statistically homogeneous among included studies. Sensitivities and specificities of all other MRI signs investigated by at least 4 studies were statistically heterogeneous ($P = 0.0189$ up to $P < 0.001$). Subgroup analyses could only be performed for some MRI signs (Table 5). For optic nerve sheath distension, diagnostic performance (expressed by the RDOR) was significantly higher in studies using "normal" volunteers vs. diagnostic performance in studies using patients with normal brain MRI findings as control subjects (RDOR: 16.14; 95% CI: 1.64–159.05; $P = 0.0225$).

Table 2
MRI interpreter(s).

Study	Interpreter(s)
Pellerin et al. [15]	Two senior neuroradiologists (5 years of experience), one radiologist and one junior radiologist
Delen et al. [18]	A neuroradiologist and two radiology residents
Morris et al. [20]	Two neuroradiologists
Carvalho et al. [21]	Three radiologists with at least 6 years of experience in neuroradiology
Zur et al. [24]	Not reported
Görkem et al. [26]	Two pediatric radiologists with 10 and 4 years of experience in interpreting pediatric MRI studies in consensus
Bialer et al. [30]	An experienced neuroradiologist (5 years of experience) in addition to two trained investigators
Ranganathan et al. [31]	Two observers
Hoffmann et al. [32]	One neuroradiologist assessed sinus vein stenosis, the observers who assessed the other criteria were not specified
Aiken et al. [33]	Two neuroradiologists
Butros et al. [34]	Two neuroradiologists
Maralani et al. [35]	Three neuroradiologists
Degnan et al. [37]	The first author of the article, under the direction of an experienced neuroradiologist
Lim et al. [38]	Pediatric neuroradiologist
Lingawi et al. [39]	Not reported
Agid et al. [41]	Three experienced neuroradiologists
Higgins et al. [43]	Two neuroradiologists
Yuh et al. [45]	Three radiologists
Farb et al. [46]	Three neuroradiologists experienced in neurovascular imaging
Brodsky et al. [47]	The second author of the article
Gass et al. [48]	An experienced neuroradiologist

Table 3
QUADAS-2 assessment results of each of the included studies.

Study	Risk of bias				Applicability concerns		
	Patient selection	Index test	Reference standard	Flow and timing	Patient selection	Index test	Reference standard
Pellerin et al. [15]	High	High	Unclear	Low	Low	Low	Low
Delen et al. [18]	High	Low	Unclear	Low	Low	Low	Low
Morris et al. [20]	High	Unclear	Unclear	Low	Low	Low	Low
Carvalho et al. [21]	High	High	Unclear	Low	Low	Low	Low
Zur et al. [24]	High	High	Unclear	Low	Low	Low	Low
Görkem et al. [26]	High	High	Unclear	Low	Low	Low	Low
Bialer et al. [30]	High	Low	Unclear	Low	Low	Low	Low
Ranganathan et al. [31]	High	High	Unclear	Low	Low	Low	Low
Hoffmann et al. [32]	High	High	Unclear	Low	Low	Low	Low
Aiken et al. [33]	High	High	Unclear	Low	Low	Low	Low
Butros et al. [34]	High	Low	Unclear	Low	Low	Low	Low
Maralani et al. [35]	High	High	Unclear	Low	Low	Low	Low
Degnan et al. [37]	High	High	Unclear	Low	Low	Low	Low
Lim et al. [38]	High	Low	Unclear	Low	Low	Low	Low
Lingawi et al. [39]	High	High	Unclear	Low	Low	Low	Low
Agid et al. [41]	High	Low	Unclear	Low	Low	Low	Low
Higgins et al. [43]	High	High	Unclear	Low	Low	Low	Low
Yuh et al. [45]	High	High	Unclear	Low	Low	Low	Low
Farb et al. [46]	High	High	Unclear	Low	Low	Low	Low
Brodsky et al. [47]	High	Low	Unclear	Low	Low	Low	Low
Gass et al. [48]	High	High	Unclear	Low	Low	Low	Low

4. Discussion

Brain MRI is routinely performed in patients clinically suspected of having IIH, but also in patients with other causes of headache [49]. It is important to discriminate patients with IIH from those without. Our systematic review showed overall high pooled specificity but low pooled sensitivity of the MRI signs "empty" sella, posterior displacement of pituitary stalk, meningoceles, posterior globe flattening, optic nerve head protrusion, optic nerve enhancement, optic nerve sheath distension, optic nerve tortuosity, slit-like ventricles, tight subarachnoid spaces, and inferior position of cerebellar tonsils. The only MRI sign with high pooled specificity and fairly high pooled sensitivity was transverse sinus stenosis.

Transverse sinus diameter has been demonstrated to correlate to invasive venous pressure gradients in patients with IIH [50] and has also been reported to increase after lumbar puncture [51,52]. Accurate assessment of transverse sinus diameter may not only be important to diagnose IIH but also to monitor treatment effect. MR venography (MRV) can be performed by gadolinium-enhanced or by non-enhanced (including time-of-flight and phase-contrast) technique. Gadolinium-enhanced MRV was applied in six [15,20,21,24,25,46] of the eight included studies which assessed transverse sinus stenosis. Non-

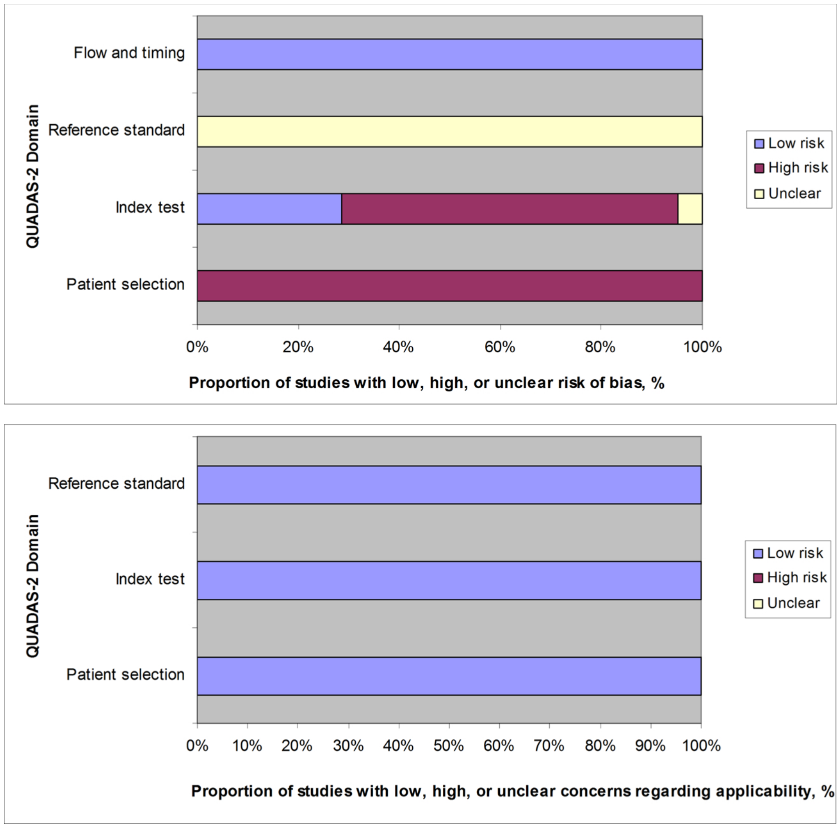

Fig. 2. Summary of QUADAS-2 assessments of the 21 included studies.

Table 4
Accuracy of MRI signs in diagnosing IIH.

MRI sign	Study	Diagnostic criterion	Individual study sensitivity (95% CI)	Individual study specificity (95% CI)	Pooled sensitivity (95% CI)	Pooled specificity (95% CI)
"Empty" sella	[18]	Pituitary occupies < 50% of pituitary fossa	43.1 (27.0-60.9)	97.6 (80.8-99.8)	62.2 (48.0-74.7)	90.7 (84.8-94.4)
	[38]		27.1 (13.4-47.1)	92.9 (74.1-98.3)		
	[20]	Pituitary occupies < 50% of pituitary fossa and	53.9 (41.8-65.5)	94.3 (87.8-97.5)		
	[35]	upper aspect is concave	64.8 (50.0, 77.2)	91.9 (77.2-97.5)		
	[26]	Pituitary gland size < 3.22 mm	63.5 (44.4-79.1)	88.7 (73.1-95.8)		
	[31]	Absolute pituitary area < 151 mm^2	95.5 (67.9-99.5)	87.5 (59.8-97.1)		
	[32]	Midsagittal pituitary gland height < 4.80 mm	86.5 (68.7-95.0)	67.3 (48.1-82.1)		
	[34]	Pituitary fossa completely filled by CSF with no visible pituitary gland	65.6 (50.9-77.7)	98.9 (90.2-99.9		
	[41]	Majority of pituitary fossa filled with CSF	27.4 (14.9-44.9)	93.9 (84.5-97.7)		
	[45]	Height of pituitary < 1/3 height of pituitary fossa	84.1 (70.1-92.3)	97.9 (82.8-99.8)		
	[47]	Pituitary occupies ≤50% of the pituitary fossa and upper aspect is concave	69.0 (47.7-84.5)	92.9 (74.1-98.3)		
Posterior displacement of pituitary stalk	[35]	Posterior displacement of pituitary stalk	39.8 (26.7-54.5)	79.5 (59.0-91.3)	41.2 (31.2-51.9)	84.0 (66.5-93.3)
	[45]		42.7 (28.8-57.8)	97.9 (82.8-99.8)		
Meningoceles	[30]	Bulging of dura matter, arachnoid and CSF into Meckel's cave or presence of meninges and CSF signal in the nasal cavity, paranasal sinuses, or mastoid air cells	11.9 (6.5-20.8)	99.4 (94.1-99.9)	9.3 (4.4-18.7)	99.2 (94.1-99.9)
	[34]	Extensions of arachnoid spaces beyond the expected margin of dural reflections predominantly occurring at the skull base	5.3 (1.715.7)	98.9 (90.2-99.9)		
Posterior globe flattening	[18]	Posterior globe flattening	63.8 (45.7-78.7)	97.6 (80.8-99.8)	56.3 (46.5-65.6)	95.3 (85.7-98.6)
	[26]		55.8 (37.2-72.9)	98.4 (86.3-99.8)		
	[32]		28.8 (15.1-48.1)	98.1 (84.0-99.8)		
	[34]		65.6 (50.9-77.7)	94.4 (83.6-98.3)		
	[35]		53.4 (39.0-67.3)	97.9 (82.8-99.8)		
	[38]		60.4 (40.8-77.2)	59.5 (38.7-77.4)		
	[41]		43.5 (27.9-60.7)	99.1 (92.1-99.9)		
	[47]		78.6 (57.4-90.9)	92.9 (74.1-98.3)		

(continued on next page)

Table 4 (*continued*)

MRI sign	Study	Diagnostic criterion	Individual study sensitivity (95% CI)	Individual study specificity (95% CI)	Pooled sensitivity (95% CI)	Pooled specificity (95% CI)
Optic nerve head protrusion	[18]	Optic nerve protrusion	32.8 (18.6-51.0)	97.6 (80.8-99.8)	29.1 (20.0-40.1)	97.0 (92.0-98.9)
	[26]		40.4 (24.0-59.3)	98.4 (86.3-99.8)		
	[35]		37.5 (24.7, 52.3)	97.1 (77.1-99.7)		
	[38]		18.8 (7.9-38.2)	97.6 (80.8-99.8)		
	[41]		4.8 (1.1-18.5)	99.1 (92.1-99.9)		
	[47]		31.0 (15.5-52.3)	92.9 (74.1-98.3)		
Optic nerve enhancement	[35]	Enhancement of the insertion of the optic nerve to the globe	3.4 (0.8-13.5)	75.0 (19.8-97.3)	13.2 (2.1-51.5)	95.9 (85.1-99.9)
	[41]	Enhancement of the optic nerve head	8.1 (2.5-22.8)	97.4 (89.4-99.4)		
	[47]	Enhancement of the prelaminar optic nerve	47.2 (26.8-68.7)	96.2 (71.7-99.6)		
Optic nerve sheath distension	[18]	Optic nerve sheath width > 2 mm	46.6 (29.9-64.0)	97.6 (80.8-99.8)	68.6 (54.8-79.7)	86.1 (78.8-91.1)
	[20]	Optic nerve sheath width > 6 mm	63.3 (51.0-74.0)	95.4 (89.2-98.1)		
	[26]	Optic nerve sheath width ≥3.61 mm	86.5 (68.7-95.0)	79.0 (61.9-89.7)		
	[32]	Maximum left optic nerve sheath diameter > 5.60 mm	78.8 (60.0-90.2)	94.2 (78.4-98.7)		
	[34]	Optic nerve sheath distension	52.2 (38.0-66.1)	87.8 (75.2-94.5)		
	[35]	Optic nerve sheath width > 2 mm	35.2 (22.8-50.0)	70.5 (49.6-85.3)		
	[37]	Optic nerve sheath diameter > 5.8 mm	86.2 (73.6-93.3)	79.8 (66.3-88.8)		
	[38]	Additive width of CSF within the midportion of the orbital optic nerve sheath > width of the optic nerve	64.6 (44.7-80.4)	64.3 (43.1-81.0)		
	[39]	Optic nerve sheath - optic nerve ratio ≥2.5	98.9 (90.4-99.9)	87.5 (66.9-96.0)		
	[41]	Optic nerve sheath width > 2 mm	66.1 (48.5-80.2)	81.6 (69.6-89.5)		
	[47]	Additive width of CSF within the midportion of the orbital optic nerve sheath > width of the optic nerve	45.2 (26.4-65.6)	92.9 (74.1-98.3)		
	[48]	Visibility of CSF ring around the optic nerve on > five 3 mm coronal T2-weighted images	97.2 (78.1-99.7)	98.9 (90.4-99.9)		
Optic nerve tortuosity	[26]	Horizontal tortuosity	40.5 (27.0-55.5)	83.3 (66.4-92.7)	36.9 (26.8-48.2)	88.4 (82.1-92.7)
	[18]	Vertical tortuosity	60.7 (42.4-76.4)	91.7 (64.6-98.5)		
	[34]		37.5 (26.7-49.7)	90.9 (78.8-96.4)		
	[35]		50.0 (35.5-64.5)	80.8 (62.1-91.5)		
	[38]		26.9 (13.7-46.1)	95.0 (76.4-99.1)		
	[41]		19.0 (11.2-30.4)	91.1 (80.7-96.1)		
	[47]		29.6 (15.9-48.5)	95.0 (76.4-99.1)		
Transverse sinus stenosis	[15]	Transverse sinus stenosis multiplicative index ≥2	98.0 (83.4-99.8)	98.0 (83.4-99.8)	84.4 (65.9-93.9)	94.9 (91.7-96.9)
	[21]	Transverse sinus stenosis index ≥4	92.4 (78.4-97.6)	92.2 (77.8-97.5)		
	[20]	Bilateral > 50% transverse sinus stenosis	93.0 (84.0-97.1)	96.4 (90.6-98.7)		
	[24]	Minimal cross-sectional area of left transverse sinus and mean cross-sectional area of right transverse sinus cut off value 55%	96.2 (84.9-99.1)	91.9 (77.2-97.5)		
	[32]	Transverse sinus stenosis	36.5 (20.9-55.6)	94.2 (78.4-98.7)		
	[35]	Combined transverse stenosis score < 4	62.5 (47.7-75.3)	98.9 (90.0-99.9)		
	[43]	Bilateral transverse sinus flow gaps	64.3 (43.1-81.0)	98.8 (89.3-99.9)		
	[46]	Combined venous conduit score ≤4.7	91.7 (76.5-97.4)	92.5 (83.0-96.9)		
Slit-like ventricles	[18]	Slit-like ventricles	5.2 (1.2-19.6)	97.6 (80.8-99.8)	14.5 (4.2-39.7)	89.9 (56.9-98.3)
	[34]		25.6 (15.1-39.9)	70.0 (55.5-81.4)		
	[35]		39.8 (26.7-54.5)	64.8 (46.0-79.9)		
	[41]		4.8 (1.1-18.5)	99.1 (92.1-99.9)		
Tight subarachnoid spaces	[18]	Very small sulci and cisterns	5.2 (1.2-19.6)	97.6 (80.8-99.8)	6.1 (2.7-13.3)	97.1 (86.7-99.4)
	[35]		8.0 (3.0-19.7)	87.5 (39.6-98.7)		
	[41]		1.6 (0.2-13.7)	99.1 (92.1-99.9)		
Inferior position of cerebellar tonsils	[18]	> 5 mm descent	8.6 (2.7-24.2)	97.6 (80.8-99.8)	19.2 (13.7-26.1)	92.8 (87.0-96.1)
	[33]	≥5 mm descent	21.6 (12.0-35.8)	96.7 (86.8-99.2)		
	[34]	Abutment of foramen magnum or ≤5 mm descent	21.1 (11.7-35.1)	90.0 (77.9-95.8)		
	[35]	> 5 mm descent	19.3 (10.3-33.2)	92.0 (80.3-97.0)		
Meckel's cave enlargement	[30]	Prominent or increased fluid signal expanding Meckel's cave but not distorting the contours	9.4 (4.7-17.7)	99.4 (94.1-99.9)	NA	NA
Meckel's cave narrowing	[37]	Maximal Meckel's cave diameter < 0.45 cm	78.3 (64.4-87.7)	84.8 (71.8-92.4)	NA	NA
Cavernous sinus diameter	[37]	Maximal cavernous sinus diameter < 0.28 cm	61.7 (47.4-74.2)	76.1 (62.1-86.1)	NA	NA
DWI bright spot at fundus	[20]	DWI bright spot at optic fundus	9.5 (4.4-19.3)	99.0 (94.3-99.8)	NA	NA
Papilledema	[20]	Papilledema	31.7 (21.6-44.4)	95.8 (89.898.4)	NA	NA

DWI: diffusion-weighted imaging.
NA: not applicable.

enhanced MRV may be susceptible to effects related to slow or turbulent flow [35]. Gadolinium-enhanced MRV does not have these disadvantages [35] but may overestimate the lumen of the transverse sinus, because the dural lining also enhances [53]. Regardless of which non-invasive imaging technique is used to detect transverse sinus stenosis, its utility may be hampered due to the high rate of venous sinus variability in normal patients [54]. Therefore, it has been suggested to use MRV (or CT venography) as a screening tool to determine candidacy for catheter venography for further analysis [54]. By measuring the pressure inside the transverse sinus before and after the stenosis area one can make sure whether or not there is a pressure gradient.

The results of this systematic review should be interpreted with caution, because there was statistically significant heterogeneity in sensitivity and specificity among the majority of MRI signs that were

Table 5
Subgroup analyses.

Parameter	Variables	MRI sign (number of studies)	Relative diagnostic odds ratio (95% CI)	*P* value
Study size	< 30 patients (5) vs. ≥30 (5)	"Empty" sella (6 vs. 5)	1.20 (0.26-5.57)	0.7926
		Posterior globe flattening (4 vs. 4)	1.81 (0.15-21.87)	0.5689
		Optic nerve sheath distension (7 vs. 5)	0.41 (0.03-5.17)	0.440
Type of control subjects	"Normal" volunteers vs. patients with normal brain MRI findings scanned for various reasons	Optic nerve sheath distension (8 vs. 4)	16.14 (1.64-159.05)	**0.0225**
Adult vs. pediatric patients with IIH	Age of included IIH patients ≥30 years vs. age of included IIH patients < 30 years	No subgroup analyses performed, because there were less than four studies per subgroup.		

investigated. All included studies had a case-control design, which may have resulted in overestimation of diagnostic accuracy [55]. In addition, inclusion of healthy controls could lead to a further overestimation of specificity. Indeed, for the MRI sign "optic nerve sheath distension", diagnostic performance was significantly higher in studies using "normal" volunteers than in studies using patients with normal brain MRI findings as control subjects. Furthermore, in 14 included studies [15,21,24,26,31–33,35,37,39,43,45,46,48] diagnostic criterion of one or more of the MRI signs was not prespecified. Accuracy is likely to be lower in an independent sample of patients in whom the same diagnostic criterion is used [9]. It is also important to note that MRI signs suggestive of elevated ICP, specifically pituitary height and globe configuration, may persist after papilledema has resolved and ICP has normalized [56]. Therefore, MRI signs of IIH should be carefully correlated with clinical findings.

Some MRI signs (Meckel's cave enlargement, Meckel's cave narrowing, cavernous sinus diameter, DWI bright spot at optic fundus, and papilledema) were only reported by single studies; their diagnostic value needs confirmation by independent studies. Only few of the included studies investigated the value of a combination of MRI signs, which yielded different results: Delen et al. [18] found that the combined criterion of either "empty" sella or posterior globe flattening achieved the highest combination of sensitivity (75%) and specificity (100%). Using this same combined criterion of either "empty" sella or posterior globe flattening, Maralani et al. [35] and Agid et al. [41] found much lower sensitivity (37.2% and 56.7%, respectively) and equally high specificity (100% and 94.6%, respectively). When Maralani et al. [35] added the MRI sign transverse sinus stenosis, sensitivity increased (86%) while maintaining high specificity (95.3%). In Degnan et al.'s study [37], the combination of Meckel's cave narrowing and optic nerve sheath distension achieved the highest combination of sensitivity (97.8%) and specificity (68.9%). In a pediatric population, Lim et al. [38] found that the presence of at least three of the MRI signs "empty" sella, posterior globe flattening, optic nerve head protrusion, optic nerve sheath distension, or optic nerve tortuosity achieved the highest sensitivity (43%) and specificity (85%). A future prospective study is needed to identify which MRI signs are independently diagnostic and which MRI signs have the highest association with IIH. A case-control design should be avoided. This will allow the development of an MRI-based prediction model for IIH, which ideally should also incorporate clinical patient parameters.

Our systematic review had some limitations. First, there were insufficient studies to explore potential sources of heterogeneity for the majority of MRI signs. We could not explore either whether diagnostic accuracy of potentially age-dependent MRI signs such as pituitary height [57,58] differs between adult and pediatric patients. Second, we did not evaluate publication bias because of low statistical power, as the number of included studies per MRI sign was relatively low. Furthermore, visual assessment of a funnel plot has questionable validity [59], whereas Deeks' test has limited utility when there is heterogeneity between studies [60].

5. Conclusions

"Empty" sella, posterior displacement of pituitary stalk, meningoceles, posterior globe flattening, optic nerve head protrusion, optic nerve enhancement, optic nerve sheath distension, optic nerve tortuosity, slit-like ventricles, tight subarachnoid spaces, and inferior position of cerebellar tonsils are MRI signs with overall high specificity but low sensitivity. Transverse sinus stenosis appears to be the most clinically useful MRI sign, because it has high specificity and fairly high sensitivity.

Conflicts of interest

All authors have no conflicts of interest to declare.

References

[1] A.K. Ball, C.E. Clarke, Idiopathic intracranial hypertension, Lancet Neurol. 5 (2006) 433–442.
[2] B.E. McGeeney, D.I. Friedman, Pseudotumor cerebri pathophysiology, Headache 54 (2014) 445–458, https://doi.org/10.1111/head.12291.
[3] F.J. Durcan, J.J. Corbett, M. Wall, The incidence of pseudotumor cerebri. Population studies in Iowa and Louisiana, Arch. Neurol. 45 (1988) 875–877.
[4] F.J. Rowe, N.J. Sarkies, The relationship between obesity and idiopathic intracranial hypertension, Int. J. Obes. Relat. Metab. Disord. 23 (1999) 54–59.
[5] NCD Risk Factor Collaboration (NCD-RisC), Trends in adult body-mass index in 200 countries from 1975 to 2014: a pooled analysis of 1698 population-based measurement studies with 19·2 million participants, Lancet 387 (2016) 1377–1396, https://doi.org/10.1016/S0140-6736(16)30054-X.
[6] D.D. Mackay, P.S. Garza, B.B. Bruce, N.J. Newman, V. Biousse, The demise of direct ophthalmoscopy: a modern clinical challenge, Neurol. Clin. Pract. 5 (2015) 150–157.
[7] A. Fisayo, B.B. Bruce, N.J. Newman, V. Biousse, Overdiagnosis of idiopathic intracranial hypertension, Neurology 86 (2016) 341–350, https://doi.org/10.1212/CPJ.0000000000000115.
[8] D.I. Friedman, G.T. Liu, K.B. Digre, Revised diagnostic criteria for the pseudotumor cerebri syndrome in adults and children, Neurology 81 (2013) 1159–1165, https://doi.org/10.1212/WNL.0b013e3182a55f17.
[9] P.F. Whiting, A.W. Rutjes, M.E. Westwood, S. Mallett, J.J. Deeks, J.B. Reitsma, M.M. Leeflang, J.A. Sterne, P.M. Bossuyt, QUADAS-2 Group. QUADAS-2: a revised tool for the quality assessment of diagnostic accuracy studies, Ann. Intern. Med. 155 (2011) 529–536, https://doi.org/10.7326/0003-4819-155-8-201110180-00009.
[10] J.B. Reitsma, A.S. Glas, A.W. Rutjes, R.J. Scholten, P.M. Bossuyt, A.H. Zwinderman, Bivariate analysis of sensitivity and specificity produces informative summary measures in diagnostic reviews, J. Clin. Epidemiol. 58 (2005) 982–990, https://doi.org/10.1016/j.jclinepi.2005.02.022.
[11] A.S. Glas, J.G. Lijmer, M.H. Prins, G.J. Bonsel, P.M. Bossuyt, The diagnostic odds ratio: a single indicator of test performance, J. Clin. Epidemiol. 56 (2003) 1129–1135.
[12] R. Fu, G. Gartlehner, M. Grant, T. Shamliyan, A. Sedrakyan, T.J. Wilt, L. Griffith, M. Oremus, P. Raina, A. Ismaila, P. Santaguida, J. Lau, T.A. Trikalinos, Conducting quantitative synthesis when comparing medical interventions: AHRQ and the Effective Health Care Program, J. Clin. Epidemiol. 64 (2011) 1187–1197, https://doi.org/10.1016/j.jclinepi.2010.08.010.
[13] https://www.r-project.org/.
[14] https://www.rdocumentation.org/packages/mada/versions/0.5.8/topics/mada-package.
[15] A. Pellerin, J. Aguilar Garcia, A. David, J. Meyer, B. Guyomarch Delasalle, S. De Gaalon, E. Auffray Calvier, H. Desal, R. Bourcier, A quantitative and semi-automatic measurement of transverse sinus stenosis improves idiopathic intracranial hypertension diagnostic accuracy, J. Neuroradiol. 45 (2018) 329–332, https://doi.org/10.1016/j.neurad.2018.05.001.
[16] J. Juhász, T. Lindner, C. Riedel, N.G. Margraf, O. Jansen, A. Rohr, Quantitative phase-contrast MR angiography to measure hemodynamic changes in idiopathic intracranial hypertension, AJNR Am. J. Neuroradiol. 39 (2018) 682–686, https://doi.org/10.3174/ajnr.A5571.
[17] G.V. Watane, B. Patel, D. Brown, M.R. Taheri, The significance of arachnoid granulation in patients with idiopathic intracranial hypertension, J. Comput. Assist. Tomogr. 42 (2018) 282–285, https://doi.org/10.1097/RCT.0000000000000668.
[18] F. Delen, E. Peker, M. Onay, C.M. Altay, O. Tekeli, C.T. Işıkay, The significance and reliability of imaging findings in pseudotumor cerebri, Neuro-Ophthalmology 43 (2018) 81–90, https://doi.org/10.1080/01658107.2018.1493514.
[19] P.P. Morris, N. Lachman, D.F. Black, R.A. Carter, J. Port, N. Campeau, Increased curvature of the tentorium cerebelli in idiopathic intracranial hypertension, AJNR Am. J. Neuroradiol. 38 (2017) 1789–1793, https://doi.org/10.3174/ajnr.A5289.
[20] P.P. Morris, D.F. Black, J. Port, N. Campeau, Transverse sinus stenosis is the most sensitive MR imaging correlate of idiopathic intracranial hypertension, AJNR Am. J. Neuroradiol. 38 (2017) 471–477, https://doi.org/10.3174/ajnr.A5289.
[21] G.B. Carvalho, S.L. Matas, M.H. Idagawa, L.A. Tibana, R.S. de Carvalho, M.L. Silva, H. Cogo-Moreira, A.P. Jackowski, N. Abdala, A new index for the assessment of transverse sinus stenosis for diagnosing idiopathic intracranial hypertension, J. Neurointerv. Surg. 9 (2017) 173–177, https://doi.org/10.1136/neurintsurg-2016-012605.
[22] A.J. Hartmann, B.P. Soares, B.B. Bruce, A.M. Saindane, N.J. Newman, V. Biousse, J.H. Peragallo, Imaging features of idiopathic intracranial hypertension in children, J. Child Neurol. 32 (2017) 120–126, https://doi.org/10.1177/0883073816671855.
[23] R. Akay, O. Kamisli, A. Kahraman, S. Oner, M. Tecellioglu, Evaluation of aqueductal CSF flow dynamics with phase contrast cine MR imaging in idiopathic intracranial hypertension patients: preliminary results, Eur. Rev. Med. Pharmacol. Sci. 19 (2015) 3475–3479.
[24] D. Zur, R. Anconina, A. Kesler, S. Lublinsky, R. Toledano, I. Shelef, Quantitative imaging biomarkers for dural sinus patterns in idiopathic intracranial hypertension, Brain Behav. 7 (2017) e00613, , https://doi.org/10.1002/brb3.613.
[25] T. Hirfanoglu, K. Aydin, A. Serdaroglu, C. Havali, Novel magnetic resonance imaging findings in children with intracranial hypertension, Pediatr. Neurol. 53 (2015) 151–156, https://doi.org/10.1016/j.pediatrneurol.2015.03.028.
[26] S.B. Görkem, S. Doğanay, M. Canpolat, G. Koc, M.S. Dogan, H. Per, A. Coşkun, MR imaging findings in children with pseudotumor cerebri and comparison with healthy controls, Childs Nerv. Syst. 31 (2015) 373–380, https://doi.org/10.1007/s00381-014-2579-0.
[27] J. Hoffmann, C. Schmidt, H. Kunte, R. Klingebiel, L. Harms, H.J. Huppertz, L. Lüdemann, E. Wiener, Volumetric assessment of optic nerve sheath and hypophysis in idiopathic intracranial hypertension, AJNR Am. J. Neuroradiol. 35 (2014) 513–518, https://doi.org/10.3174/ajnr.A3694.
[28] S.E. Kyung, J.V. Botelho, J.C. Horton, Enlargement of the sella turcica in pseudotumor cerebri, J. Neurosurg. 120 (2014) 538–542, https://doi.org/10.3171/2013.10.JNS131265.
[29] M.A. Ridha, A.M. Saindane, B.B. Bruce, B.D. Riggeal, L.P. Kelly, N.J. Newman, V. Biousse, MRI findings of elevated intracranial pressure in cerebral venous thrombosis versus idiopathic intracranial hypertension with transverse sinus stenosis, Neuroophthalmology 37 (2013) 1–6, https://doi.org/10.3109/01658107.2012.738759.
[30] O.Y. Bialer, M.P. Rueda, B.B. Bruce, N.J. Newman, V. Biousse, A.M. Saindane, Meningoceles in idiopathic intracranial hypertension, AJR Am. J. Roentgenol. 202 (2014) 608–613, https://doi.org/10.2214/AJR.13.10874.
[31] S. Ranganathan, S.H. Lee, A. Checkver, E. Sklar, B.L. Lam, G.H. Danton, N. Alperin, Magnetic resonance imaging finding of empty sella in obesity related idiopathic intracranial hypertension is associated with enlarged sella turcica, Neuroradiology 55 (2013) 955–961, https://doi.org/10.1007/s00234-013-1207-0.
[32] J. Hoffmann, H.J. Huppertz, C. Schmidt, H. Kunte, L. Harms, R. Klingebiel, E. Wiener, Morphometric and volumetric MRI changes in idiopathic intracranial hypertension, Cephalalgia 33 (2013) 1075–1084, https://doi.org/10.1177/0333102413484095.
[33] A.H. Aiken, J.A. Hoots, A.M. Saindane, P.A. Hudgins, Incidence of cerebellar tonsillar ectopia in idiopathic intracranial hypertension: a mimic of the Chiari I malformation, AJNR Am. J. Neuroradiol. 33 (2012) 1901–1906, https://doi.org/10.3174/ajnr.A3068.
[34] S.R. Butros, L.F. Goncalves, D. Thompson, A. Agarwal, H.K. Lee, Imaging features of idiopathic intracranial hypertension, including a new finding: widening of the foramen ovale, Acta Radiol. 53 (2012) 682–688, https://doi.org/10.1258/ar.2012.110705.
[35] P.J. Maralani, M. Hassanlou, C. Torres, S. Chakraborty, M. Kingstone, V. Patel, D. Zackon, M. Bussière, Accuracy of brain imaging in the diagnosis of idiopathic intracranial hypertension, Clin. Radiol. 67 (2012) 656–663, https://doi.org/10.1016/j.crad.2011.12.002.
[36] B. Shofty, L. Ben-Sira, S. Constantini, S. Freedman, A. Kesler, Optic nerve sheath diameter on MR imaging: establishment of norms and comparison of pediatric patients with idiopathic intracranial hypertension with healthy controls, AJNR Am. J. Neuroradiol. 33 (2012) 366–369, https://doi.org/10.3174/ajnr.A2779.
[37] A.J. Degnan, L.M. Levy, Narrowing of Meckel's cave and cavernous sinus and enlargement of the optic nerve sheath in pseudotumor cerebri, J. Comput. Assist. Tomogr. 35 (2011) 308–312, https://doi.org/10.1097/RCT.0b013e31820d7a70.
[38] M.J. Lim, K. Pushparajah, W. Jan, D. Calver, J.P. Lin, Magnetic resonance imaging changes in idiopathic intracranial hypertension in children, J. Child Neurol. 25 (2010) 294–299, https://doi.org/10.1177/0883073809338874.
[39] S.S. Lingawi, Magnetic resonance imaging measurements of optic sheath to optic nerve diameter ratio for the diagnosis of idiopathic intracranial hypertension, J. HK Coll. Radiol. 12 (2010) 103–106.
[40] K. Bicakci, S. Bicakci, E. Aksungur, Perfusion and diffusion magnetic resonance imaging in idiopathic intracranial hypertension, Acta Neurol. Scand. 114 (2006) 193–197, https://doi.org/10.1111/j.1600-0404.2006.00702.x.
[41] R. Agid, R.I. Farb, R.A. Willinsky, D.J. Mikulis, G. Tomlinson, Idiopathic intracranial hypertension: the validity of cross-sectional neuroimaging signs, Neuroradiology 48 (2006) 521–527, https://doi.org/10.1007/s00234-006-0095-y.
[42] S.S. Lingawi, S.S. Baeesa, H.A. Al-Gahtani, Brain versus orbital MRI in evaluating idiopathic intracranial hypertension, Neurosciences (Riyadh) 10 (2005) 76–78.
[43] J.N. Higgins, J.H. Gillard, B.K. Owler, K. Harkness, J.D. Pickard, MR venography in idiopathic intracranial hypertension: unappreciated and misunderstood, J. Neurol. Neurosurg. Psychiatry 75 (2004) 621–625.
[44] M.E. Bastin, S. Sinha, A.J. Farrall, J.M. Wardlaw, I.R. Whittle, Diffuse brain oedema in idiopathic intracranial hypertension: a quantitative magnetic resonance imaging study, J. Neurol. Neurosurg. Psychiatry 74 (2003) 1693–1696.
[45] W.T. Yuh, M. Zhu, T. Taoka, J.P. Quets, J.E. Maley, M.G. Muhonen, M.E. Schuster, R.H. Kardon, MR imaging of pituitary morphology in idiopathic intracranial hypertension, J. Magn. Reson. Imaging 12 (2000) 808–813.
[46] R.I. Farb, I. Vanek, J.N. Scott, D.J. Mikulis, R.A. Willinsky, G. Tomlinson, K.G. terBrugge, Idiopathic intracranial hypertension: the prevalence and morphology of sinovenous stenosis, Neurology 60 (2003) 1418–1424.
[47] M.C. Brodsky, M. Vaphiades, Magnetic resonance imaging in pseudotumor cerebri, Ophthalmology 105 (1998) 1686–1693.
[48] A. Gass, G.J. Barker, P. Riordan-Eva, D. MacManus, M. Sanders, P.S. Tofts, W.I. McDonald, I.F. Moseley, D.H. Miller, MRI of the optic nerve in benign intracranial hypertension, Neuroradiology 38 (1996) 769–773.
[49] B.C. Callaghan, K.A. Kerber, R.J. Pace, L. Skolarus, W. Cooper, J.F. Burke, Headache neuroimaging: routine testing when guidelines recommend against them, Cephalalgia 35 (2015) 1144–1152, https://doi.org/10.1177/0333102415572918.
[50] J.L. West, G.P. Greeneway, R.M. Garner, C.A. Aschenbrenner, J. Singh, S.Q. Wolfe, K.M. Fargen, Correlation between angiographic stenosis and physiologic venous sinus outflow obstruction in idiopathic intracranial hypertension, J. Neurointerv. Surg. 11 (2019) 90–94, https://doi.org/10.1136/neurintsurg-2018-014004.
[51] A. Horev, H. Hallevy, Y. Plakht, Z. Shorer, I. Wirguin, I. Shelef, Changes in cerebral venous sinuses diameter after lumbar puncture in idiopathic intracranial hypertension: a prospective MRI study, J. Neuroimaging 23 (2013) 375–378, https://doi.org/10.1111/j.1552-6569.2012.00732.x.
[52] T.J. Buell, D.M.S. Raper, I.J. Pomeraniec, D. Ding, C.J. Chen, D.G. Taylor, K.C. Liu, Transient resolution of venous sinus stenosis after high-volume lumbar puncture in

a patient with idiopathic intracranial hypertension, J. Neurosurg. 129 (2018) 153–156, https://doi.org/10.3171/2017.3.JNS163181.
[53] S.R. Boddu, P. Gobin, C. Oliveira, M. Dinkin, A. Patsalides, Anatomic measurements of cerebral venous sinuses in idiopathic intracranial hypertension patients, PLoS One 13 (2018) e0196275, , https://doi.org/10.1371/journal.pone.0196275.
[54] K.M. Fargen, K. Liu, R.M. Garner, G.P. Greeneway, S.Q. Wolfe, R.W. Crowley, Recommendations for the selection and treatment of patients with idiopathic intracranial hypertension for venous sinus stenting, J. Neurointerv. Surg. 10 (2018) 1203–1208, https://doi.org/10.1136/neurintsurg-2018-01404.
[55] J.G. Lijmer, B.W. Mol, S. Heisterkamp, G.J. Bonsel, M.H. Prins, J.H. van der Meulen, P.M. Bossuyt, Empirical evidence of design-related bias in studies of diagnostic tests, JAMA 282 (1999) 1061–1066.
[56] R.O. Chang, B.K. Marshall, N. Yahyavi, A. Sharma, J. Huecker, M.O. Gordon, C. McClelland, G.P. Van Stavern, Neuroimaging features of idiopathic intracranial hypertension persist after resolution of papilloedema, Neuroophthalmology 40 (2016) 165–170, https://doi.org/10.1080/01658107.2016.1179767.
[57] A. Tsunoda, O. Okuda, K. Sato, MR height of the pituitary gland as a function of age and sex: especially physiological hypertrophy in adolescence and in climacterium, AJNR Am. J. Neuroradiol. 18 (1997) 551–554.
[58] A. Rohr, C. Riedel, G. Reimann, K. Alfke, J. Hedderich, O. Jansen, Pseudotumor cerebri: quantitative in-vivo measurements of markers of intracranial hypertension, Rofo 180 (2008) 884–890, https://doi.org/10.1055/s-2008-1027627.
[59] N. Terrin, C.H. Schmid, J. Lau, In an empirical evaluation of the funnel plot, researchers could not visually identify publication bias, J. Clin. Epidemiol. 58 (2005) 894–901, https://doi.org/10.1016/j.jclinepi.2005.01.006.
[60] M.D. McInnes, P.M. Bossuyt, Pitfalls of systematic reviews and meta-analyses in imaging research, Radiology 277 (2015) 13–21, https://doi.org/10.1148/radiol.2015142779.
[61] D.I. Friedman, E.A. Rausch, Headache diagnoses in patients with treated idiopathic intracranial hypertension, Neurology 58 (2002) 1551–1553.
[62] Headache Classification Subcommittee of the International Headache Society, The international classification of headache disorders, 2nd edition, Cephalalgia 24 (Suppl) (2004) 9–160.